

Remote Sensing for Vegetation Monitoring

Technologies, Applications and Models

Edited by
Prem Chandra Pandey
Mukunda Dev Behera
Komali Kantamaneni
Navneet Kumar

ELSEVIER

Remote Sensing for Vegetation Monitoring

Technologies, Applications and Models

Remote Sensing for Vegetation Monitoring

Technologies, Applications and Models

Edited by

Prem Chandra Pandey

Department of Life Sciences, School of Natural Sciences,
Shiv Nadar Institution of Eminence(Deemed to be University), Greater Noida, Uttar Pradesh, India

Mukunda Dev Behera

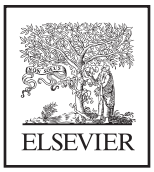
Centre for Oceans, Rivers, Atmosphere and Land Sciences (CORAL),
Indian Institute of Technology Kharagpur, Kharagpur, West Bengal, India

Komali Kantamaneni

Faculty of Science and Technology, University of Central Lancashire (UCLan),
Preston, Lancashire, United Kingdom

Navneet Kumar

Ecology and Natural Resources Management Division,
Center for Development Research (ZEF), Bonn, Germany



Elsevier
Radarweg 29, PO Box 211, 1000 AE Amsterdam, Netherlands
125 London Wall, London EC2Y 5AS, United Kingdom
50 Hampshire Street, 5th Floor, Cambridge, MA 02139, United States

Copyright © 2027 Elsevier Inc. All rights are reserved, including those for text and data mining, AI training, and similar technologies.

For accessibility purposes, images in electronic versions of this book are accompanied by alt text descriptions independently provided by Elsevier, generated with the aid of AI. For more information, see https://www.elsevier.com/about/accessibility or Radarweg 29, 1043 NX Amsterdam, Netherlands.

Books and Journals published by Elsevier comply with applicable product safety requirements. For any product safety concerns or queries, please contact our authorised representative, Elsevier B.V., at productsafety@elsevier.com.

Publisher's note: Elsevier takes a neutral position with respect to territorial disputes or jurisdictional claims in its published content, including in maps and institutional affiliations.

No part of this publication may be reproduced or transmitted in any form or by any means, electronic or mechanical, including photocopying, recording, or any information storage and retrieval system, without permission in writing from the publisher. Details on how to seek permission, further information about the Publisher's permissions policies and our arrangements with organizations such as the Copyright Clearance Center and the Copyright Licensing Agency, can be found at our website: www.elsevier.com/permissions.

This book and the individual contributions contained in it are protected under copyright by the Publisher (other than as may be noted herein).

Notices
Knowledge and best practice in this field are constantly changing. As new research and experience broaden our understanding, changes in research methods, professional practices, or medical treatment may become necessary.

Practitioners and researchers must always rely on their own experience and knowledge in evaluating and using any information, methods, compounds, or experiments described herein. In using such information or methods they should be mindful of their own safety and the safety of others, including parties for whom they have a professional responsibility.

To the fullest extent of the law, neither the Publisher nor the authors, contributors, or editors, assume any liability for any injury and/or damage to persons or property as a matter of products liability, negligence or otherwise, or from any use or operation of any methods, products, instructions, or ideas contained in the material herein.

ISBN: 978-0-443-33076-6

For information on all Elsevier publications visit our website at https://www.elsevier.com/books-and-journals

Publisher: Peter Llewellyn
Acquisitions Editor: Menka Mehta
Editorial Project Manager: Namrata Aggarwal
Production Project Manager: Anitha Sivaraj
Cover Designer: Arumugam Kothandan

Printed in England by CPI Group (UK) Ltd
Croydon CRo 4YY
United Kingdom

Typeset by Integra Software Services



Contributors

Ruchi Bala Department of Physics, D. K. College, Dumraon, Buxar, India

Mukunda Dev Behera Centre for Ocean, River, Atmosphere and Land Sciences, Indian Institute of Technology Kharagpur, Kharagpur, West Bengal, India

Mahadev Bera School of Environment and Disaster Management, Ramakrishna Mission Vivekananda Educational and Research Institute, Kolkata, West Bengal, India

Amnat Chidthaisong The Joint Graduate School of Energy and Environment (JGSEE), King Mongkut's University of Technology Thonburi (KMUTT), Bangkok, Thailand

Sumanta Das School of Environment and Disaster Management, Ramakrishna Mission Vivekananda Educational and Research Institute, Kolkata, West Bengal, India

Cátia Rodrigues de Almeida Faculty of Sciences, Department of Geosciences, Environment and Land Planning, University of Porto; Institute of Earth Sciences (ICT), Porto; CIMO, LA SusTEC, Universidade Politécnica de Bragança, Bragança, Portugal

Nguyen Thi Hong Diep College of Environment and Natural Resources, Can Tho University, Can Tho City, Vietnam

Lia Duarte Department of Geosciences, Environment and Spatial Planning; Institute of Earth Sciences, Faculty of Sciences, University of Porto, Porto, Portugal

Timothy Dube Institute for Water Studies, Department of Earth Sciences, University of the Western Cape, Bellville, South Africa

Suman Dutta Department of Genetics and Plant Breeding, Ramakrishna Mission Vivekananda Educational and Research Institute, Kolkata, West Bengal, India

Chandra Shekhar Dwivedi Department of Geinformatics, Central University of Jharkhand, Ranchi, India

Chaiwat Ekkawatpanit Faculty of Engineering, King Mongkut's University of Technology Thonburi (KMUTT), Bangkok, Thailand

Artur Gonçalves CIMO, LA SusTEC, Universidade Politécnica de Bragança, Bragança, Portugal

N.S. Gudmewad Agricultural and Food Engineering Department, IIT Kharagpur, Kharagpur, India

R. Hebbar Regional Remote Sensing Centre-South, National Remote Sensing Centre (NRSC), Indian Space Research Organisation (ISRO), ISITE Campus, Bengaluru, Karnataka, India

Saahil Hembrom Department of Civil and Environmental Engineering, Birla Institute of Technology, Mesra, Ranchi, Jharkhand, India

C. Jeganathan Department of Remote Sensing, Birla Institute of Technology (BIT), Mesra; Sarala Birla University, Ranchi, Jharkhand, India

R. Joshi Regional Centre, GBP-NIHE, Gangtok, Sikkim, India

Komali Kantamaneni School of Engineering and Computing, University of Lancashire; UN SPIDER-UK, Regional Support Office, Preston, United Kingdom

Navneet Kumar Center for Development Research (ZEF), University of Bonn, Ecology and Natural Resources Management; Divison of Ecology and Natural Resources Management, University of Bonn, Center for Development Research (ZEF), Bonn, Germany; National Institute of Disaster Management (NIDM), Ministry of Home Affairs, Government of India, Vijayawada, India

Neeta Kumari Department of Civil and Environmental Engineering, Birla Institute of Technology, Mesra, Ranchi, Jharkhand, India

Nikhil Lele EPSA, Space Applications Centre (SAC), ISRO, Ahmedabad, Gujarat, India

Atsamon Limsakul Climate Change and Environmental Research Center, Pathumthani, Thailand

Anita Masenyama Discipline of Geography, School of Agriculture and Science, University of KwaZulu-Natal, Pietermaritzburg, Scottsville, South Africa

Jincy Rachel Mathew EPSA, Space Applications Centre (SAC), ISRO; Department of Environmental Sciences, Gujarat University, Ahmedabad, Gujarat, India

R. Maurya School of Water Resources, IIT Kharagpur, Kharagpur, India

A. Mishra Agricultural and Food Engineering Department, IIT Kharagpur, Kharagpur, India

Onisimo Mutanga Discipline of Geography, School of Agriculture and Science, University of KwaZulu-Natal, Pietermaritzburg, Scottsville, South Africa

Manish Kumar Naskar Department of Agricultural Meteorology and Physics, Bidhan Chandra Krishi Viswavidyalaya, Mohanpur, India

Can Trong Nguyen Environment Centre, Charles University, Prague, Czech Republic; The Joint Graduate School of Energy and Environment (JGSEE), King Mongkut's University of Technology Thonburi (KMUTT), Bangkok, Thailand

Prem Chandra Pandey Department of Life Sciences, School of Natural Sciences, Shiv Nadar Institution of Eminence (Deemed to be University), Greater Noida, Uttar Pradesh, India

Soumya Pandey Department of Civil Engineering, Lingaya's Vidyapeeth, Faridabad, Haryana, India

Wankhede Mahendra Pandhari Centre for Ocean, River, Atmosphere and Land Sciences, Indian Institute of Technology Kharagpur, Kharagpur, West Bengal, India

Rajendra Prasad Department of Physics, Indian Institute of Technology (BHU), Varanasi, India

Iraj Rahimi Department of Geosciences, Environment and Spatial Planning; Institute of Earth Sciences, Faculty of Sciences, University of Porto, Porto, Portugal; Darbandikhan Technical Institute, Sulaimani Polytechnic University, Sulaymaniyah, Iraq

Malini Roy Choudhury School of Environment and Disaster Management, Ramakrishna Mission Vivekananda Educational and Research Institute, Kolkata, West Bengal, India

Manali Santra Department of Geoinformatics, Central University of Jharkhand, UGC-SRF, Ranchi, India

Dhruvi Sedha EPSA, Space Applications Centre (SAC), ISRO; Department of Environmental Sciences, Gujarat University, Ahmedabad, Gujarat, India

Aliihsan Sekertekin Department of Architecture and Town Planning, Igdir University, Igdir, Turkey

Mbulisi Sibanda Department of Geography, Environmental Studies & Tourism, Faculty of Arts, University of the Western Cape, Bellville, South Africa

C.P. Singh EPSA, Space Applications Centre (SAC), ISRO, Ahmedabad, India

Chandra Prakash Singh EPSA, Space Applications Centre (SAC), ISRO, Ahmedabad, Gujarat, India

S.P. Singh Amity Institute of GeoInformatics and Remote Sensing, Amity University Uttar Pradesh, Noida, India

Sumedha Surbhi Singh Department of Remote Sensing, Birla Institute of Technology (BIT), Mesra, Ranchi, India

Suman Sinha Department of Geography, Amity University, Kolkata, India

S. Sinki Centre for Ocean, River, Atmosphere and Land Sciences, Indian Institute of Technology Kharagpur, Kharagpur, West Bengal, India

Hitesh Solanki Department of Environmental Sciences, Gujarat University, Ahmedabad, Gujarat, India

C. Sudhakar Reddy Forest Biodiversity and Ecology Division, NRSC, Hyderabad, Telangana, India

Ana Teodoro CIMO, LA SusTEC, Universidade Politécnica de Bragança, Bragança, Portugal

Ana Cláudia Teodoro Department of Geosciences, Environment and Spatial Planning; Institute of Earth Sciences, Faculty of Sciences, University of Porto, Porto, Portugal

Shivam Trivedi Regional Remote Sensing Centre-South, National Remote Sensing Centre (NRSC), Indian Space Research Organisation (ISRO), ISITE Campus, Bengaluru, Karnataka, India

Jyoti Verma Department of Zoology, CMP College, University of Allahabad, Prayagraj, India

P.V. Vinod Regional Remote Sensing Centre-South, National Remote Sensing Centre (NRSC), Indian Space Research Organisation (ISRO), ISITE Campus, Bengaluru, Karnataka, India

Vijay Pratap Yadav Department of Physics, Government Degree College, Gahmar, Ghazipur, India

Sevim Seda Yamaç Department of Biosystems Engineering, Necmettin Erbakan University, Eregli Faculty of Agriculture, Konya, Turkey

Rahat Zehra Geospatial Information Science and Engineering Hub, Indian Institute of Technology Bombay, Powai, India

Foreword

It is my pleasure to contribute this foreword to the Book entitled **"***Remote Sensing for Vegetation Monitoring: Technologies, Applications and Models"* (First Edition, Elsevier), **edited by Drs. Prem Chandra Pandey, Mukunda Dev Behera, Komali Kantamaneni, and Navneet Kumar,** an emerging group of scholars whose work reflects the growing sophistication and global relevance of vegetation remote sensing. Vegetation forms the structural and functional backbone of terrestrial ecosystems, shaping biodiversity, hydrological processes, climate regulation, and agricultural productivity. As global environmental change accelerates, the demand for accurate, timely, and scalable vegetation monitoring has become central to scientific research, environmental governance, and sustainable development. This volume offers a comprehensive and authoritative synthesis of contemporary advances in satellite-based vegetation assessment, serving as a valuable reference for researchers, practitioners, and policymakers engaged in environmental monitoring and land-resource management.

The strength of this book lies in its breadth, depth, and thematic coherence. The editors have curated contributions from leading experts whose work spans forests, mangroves, agricultural systems, grasslands, and urban environments. Across 18 chapters, the volume demonstrates how rapid advances in Earth observation technologies, combined with machine learning, cloud computing, and multi-sensor data fusion, are transforming our capacity to observe, quantify, and model vegetated landscapes at multiple spatial and temporal scales.

Section II, the most extensive section, provides a rigorous examination of forest ecosystem monitoring. The opening chapter traces five decades of progress in India's Earth observation programs, documenting the transition from manual interpretation to AI-enabled analytical frameworks capable of supporting national-scale vegetation databases. Subsequent chapters highlight the power of long-term MODIS time series for biodiversity modeling, the utility of vegetation indices for detecting ecosystem stress, and the unique advantages of Sentinel-1 SAR for retrieving crop biophysical parameters under all-weather conditions. The section also presents emerging methodologies, including automated digital phenology using machine learning, multi-sensor fire-risk assessment in semi-arid and semi-Mediterranean regions, and hydrological modeling that underscores the role of forests and rangelands in sustaining watershed stability. Collectively, these contributions illustrate the expanding methodological

toolkit available for forest monitoring and the importance of integrating optical, radar, and digital imagery for comprehensive ecosystem assessment.

Section III focuses on mangrove ecosystems, critical coastal buffers increasingly threatened by climate extremes and anthropogenic pressures. The chapters document the impacts of Cyclone Amphan on the Sundarbans and present two decades of Landsat-based mangrove change analysis across India's coastal states. These studies reveal spatially heterogeneous patterns of degradation and recovery, emphasizing the need for continuous satellite-based monitoring to support conservation, climate mitigation, and progress toward Sustainable Development Goals.

Section IV turns to agricultural monitoring, an area where remote sensing has become indispensable for addressing global food and water security. The chapters demonstrate how high-resolution satellite and UAV imagery support irrigation management, crop damage assessment, and climate-resilient agricultural planning. Multi-sensor fusion, combining optical, SAR, thermal, UAV, and AI-driven analytics, emerges as a powerful approach for improving crop health assessment, insurance evaluation, and disaster response. The section also highlights the transformative potential of AI-enabled geospatial intelligence for agricultural monitoring in developing regions, where soil, water, and land-reclamation challenges require integrated, data-driven solutions.

Section V provides an in-depth exploration of grassland and rangeland monitoring. The chapters illustrate how hyperspectral data, particularly red-edge and SWIR bands, combined with machine learning, enable accurate estimation of grass quality and biochemical properties. A comprehensive overview of remote sensing techniques for tracking grassland phenology, biomass, and species composition underscores the importance of these ecosystems for biodiversity conservation, carbon sequestration, and climate adaptation.

Section VI addresses vegetation monitoring in urban environments, where green spaces play a vital role in mitigating heat stress and enhancing urban livability. The chapters present empirical evidence of the cooling benefits of urban parks, the influence of green-space structure on land surface temperature, and the utility of cloud-based platforms such as Google Earth Engine for automated vegetation, water, and temperature analysis. These contributions offer practical insights for climate-responsive urban planning and sustainable city design.

Across its six sections, this volume demonstrates remarkable progress in remote sensing technologies and analytical methods for vegetation monitoring. It highlights the convergence of multi-sensor satellite missions, advanced computational models, and cloud-scale processing environments—developments that collectively enable unprecedented global environmental intelligence. The case studies span diverse biomes and climatic regions, illustrating how remote sensing supports conservation, climate adaptation, agricultural resilience, and sustainable development.

Remote Sensing for Vegetation Monitoring: Technologies, Applications and Models **by Dr. Prem Pandey et al.** stands as a timely and significant contribution to the field. It will serve as an essential reference for scholars, practitioners, and policymakers seeking to understand and apply state-of-the-art remote sensing techniques for vegetation assessment. The editors and contributors are to be commended for producing a volume that not only synthesizes current knowledge but also charts a clear path for future research and innovation in vegetation monitoring.



Dr. Prasad S. Thenkabail, PhD

Senior Scientist, U. S. Geological Survey (USGS)
USA

Preface

The motivation for compiling *Remote Sensing for Vegetation Monitoring* is based on the understanding that vegetation systems are both indicators and regulators of environmental change. Vegetation responds rapidly to climatic variability, anthropogenic disturbances, and land-use transformations, making it a critical component for assessing ecosystem health and resilience. Traditional field-based methods, while indispensable, are often constrained by scale, cost, and temporal limitations. Remote sensing, combined with geospatial analysis and data-driven models, provides an effective way to address these limitations.

This book brings together contributions from experts across diverse disciplines and regions to provide an integrated perspective on vegetation monitoring using remote sensing. This multi-authored volume consists of 18 thoughtfully organised chapters following an introductory editorial chapter and theme-based chapters. The chapters span foundational concepts, methodological advancements, and applied case studies, highlighting the recent developments in Earth observation technologies. Readers will find discussions on long-term satellite time-series analysis, vegetation indices, phenological monitoring, polarimetric SAR applications, hyperspectral assessments of vegetation quality, and the integration of machine learning and cloud-based platforms for automated analysis.

A distinctive feature of this volume is its balanced focus on natural and managed ecosystems. Forests, grasslands, mangroves, semi-arid landscapes, mountain watersheds, agricultural fields, and urban green spaces are examined using tailored remote sensing approaches. Several chapters emphasize multi-sensor and multi-scale integration, demonstrating how optical, radar, thermal, UAV, and ground-based observations can be effectively combined to improve accuracy and reliability.

The book also highlights emerging technologies, new challenges and future directions in vegetation monitoring, including data scarcity in complex terrains, sensor limitations, scale mismatches, and the need for near-real-time information for decision-making. Advances in artificial intelligence, cloud computing, hyperspectral missions, and participatory monitoring are discussed as potential approaches to address the issues.

The chapters in this volume collectively advance the United Nations Sustainable Development Goals (SDGs) by showcasing the application of remote sensing, geospatial technologies,

artificial intelligence, and Earth observation for sustainable vegetation monitoring and mapping. This book contributes to SDG 15 (Life on Land) through ecosystem and biodiversity monitoring; SDG 13 (Climate Action) through climate resilience and disaster assessment; SDG 2 (Zero Hunger) through precision agriculture and crop monitoring; SDG 6 (Clean Water and Sanitation) through watershed and water resource management; SDG 11 (Sustainable Cities and Communities) through urban green space assessment; SDG 14 (Life Below Water) through mangrove conservation; and SDG 9 (Industry, Innovation and Infrastructure) by promoting advanced geospatial and AI-driven technologies for informed environmental decision-making and sustainable development. The focus of the book is vegetation types and their mapping, monitoring, and applications across relevant themes, with particular emphasis on their presence in particular ecosystems.

This volume is intended to serve as both a reference and a learning resource. It is expected to be useful for students and researchers, while also providing practical insights for practitioners and policymakers involved in evidence-based planning and sustainable resource management. Ultimately, this book aims to enhance understanding of vegetation systems and promote remote sensing technologies for mapping and monitoring, for a more resilient and sustainable future.

Editors

Prem Chandra Pandey New Delhi, India
Mukunda Dev Behera Kharagpur, India
Navneet Kumar Bonn, Germany
Komali Kantamaneni Lancashire, United Kingdom

CHAPTER 16

Quantifying cooling effects of urban green spaces: An empirical study from primary parks in Bangkok metropolis

Can Trong Nguyen[a,b], Amnat Chidthaisong[b], Atsamon Limsakul[c], Chaiwat Ekkawatpanit[d], and Nguyen Thi Hong Diep[e]

[a]*Environment Centre, Charles University, Prague, Czech Republic*
[b]*The Joint Graduate School of Energy and Environment (JGSEE), King Mongkut's University of Technology Thonburi (KMUTT), Bangkok, Thailand*
[c]*Climate Change and Environmental Research Center, Pathumthani, Thailand*
[d]*Faculty of Engineering, King Mongkut's University of Technology Thonburi (KMUTT), Bangkok, Thailand*
[e]*College of Environment and Natural Resources, Can Tho University, Can Tho City, Vietnam*

1 Introduction

Rapid urbanization in Thailand has occurred through both population growth and urban spatial expansion (Nguyen et al., 2021a). The development of cities, especially Bangkok megacity, induces variations in thermal environment and formation of urban heat islands (UHI) (Nguyen et al., 2023; Estoque et al., 2017; Khamchiangta and Dhakal, 2020; Nguyen et al., 2022). The UHI effects in Bangkok are particularly severe due to a combination of different factors ranging from physical to nonphysical aspects, including sky view factors, aspect ratio, building height, impervious surfaces, albedo, population density, and anthropogenic heat (Khamchiangta and Dhakal, 2019; Nguyen et al., 2025). UHI can negatively induce air pollution, low water quality, and changes in local ecosystems (Piracha and Chaudhary, 2022; Vujovic et al., 2021). It also raises energy consumption for cooling demand, as well as negative impacts on human health and wellbeing (Nguyen et al., 2021b; Piracha and Chaudhary, 2022; Singh et al., 2020). The most significant impacts on human health are disproportionately felt by vulnerable populations, such as the elderly, young children, and low-income communities (Nguyen et al., 2024a; Abrar et al., 2022; Räsänen et al., 2019). Climate change and heat waves with prolonged periods

Remote Sensing for Vegetation Monitoring. https://doi.org/10.1016/B978-0-443-33076-6.00023-4
Copyright © 2027 Elsevier Inc. All rights are reserved,
including those for text and data mining, AI training, and similar technologies.

of high temperatures can lead to heat exhaustion, dehydration, and increased heat-related mortality (Chaston et al., 2022). It is ultimately a socio-economic burden, such as decreased workers' productivity, increased health care and related costs. The negative impacts of UHI in cities are a growing concern that needs effective strategies for mitigating negative impacts and improving urban dwellers' wellbeing.

Among a slew of interventions to mitigate UHI, urban green spaces (UGS) and urban parks are increasingly recognized as effective and economical approaches. They provide a variety of benefits to urban environments and residents, such as reducing noise and air pollution, enhancing biodiversity, and providing numerous intangible values as ecosystem services (Nguyen and Chidthaisong, 2023). One of the most important values that urban dwellers directly recognize is temperature reduction, which is based on the negative relationship between vegetation density and surface temperatures (Estoque and Murayama, 2017; Son et al., 2017; Wang et al., 2018). For instance, UGS can reduce air temperature by approximately 1°C–2°C around their areas (Aram et al., 2019; Kraemer and Kabisch, 2022). Yet, the cooling effect varies depending on many factors, such as background climate, park characteristics, and even surrounding landscapes (Jaganmohan et al., 2016). Key aspects of urban cooling research include the assessment of the park cooling effect, controlling factors, and park design to optimize the cooling capacity (Blachowski and Hajnrych, 2021). Previous studies mainly investigated the cooling effect from the perspective of Earth observation by considering changes in land surface temperature (LST) with distance from the boundary of UGS (Cheng et al., 2015; Qiu and Jia, 2020). It is apparent that LST dramatically shifts from inside to outside the park's boundary as LST is highly sensitive to surface properties. LST changes at park boundaries are often sharp and clear; therefore, they can easily lead to uncertainties, biases, and underestimation of the cooling effect. On the other hand, near-surface air temperature can potentially overcome these challenges in cooling effect assessment, and it is more associated with human health and wellbeing than LST. The cooling capacity of UGS mainly depends on the parks' land use and land cover (LULC) and configurations. Current studies frequently compare the cooling effect of one park against another directly. It should be noted that their surrounding areas might be very different. There are also dissimilarities in temperature, humidity, and other environmental variables that control the cooling effects. In other words, it is hard to find two parks with identical neighboring areas to compare the impact of their features on the cooling effects. In this case, modeling is a promising approach that puts parks under the same conditions to simulate their cooling effects without influence from these variations. It can facilitate cross-comparison and more objectively suggest which park characteristics are beneficial to urban cooling.

Modeling approaches have increasingly been adopted to evaluate urban cooling effects, rather than using direct Earth observation data, by integrating LULC characteristics with biophysical processes. Although high-resolution microclimate simulations, such as computational fluid dynamics approaches and urban climate models (e.g., ENVI-met), can provide highly detailed

characteristics of airflow dynamics, radiation exchanges, and fine-scale thermal processes, they typically require extensive meteorological inputs, detailed three-dimensional urban morphology data, and intensive calibration procedures. These requirements often limit their feasibility for studies covering multiple study sites and broader extents. Among the models, InVEST (Integrated Valuation of Ecosystem Services and Tradeoffs) urban cooling model (InVEST-UCM) has gained considerable attention as a spatially explicit tool for assessing temperature mitigation provided by urban green infrastructure as a kind of ecosystem service. It considers LULC as a primary proxy for generating temperature reduction service through biophysical mechanisms, including shade provision, evapotranspiration, and surface albedo variations. Previous studies have successfully applied InVEST-UCM across diverse climatic conditions and urban contexts to evaluate cooling services of green and blue spaces, investigate the influences of landscape configuration, and support urban planning and climate adaptation strategies (Zaid et al., 2025; Ronchi et al., 2020; Hu et al., 2023; Zawadzka et al., 2021; Chung et al., 2024). Its ability to standardize environmental assumptions while isolating landscape characteristics makes the model particularly suitable for comparative assessments of urban green spaces under controlled conditions.

This chapter, therefore, simulated park cooling effects using InVEST-UCM by taking LULC as a primary proxy for assessing cooling performance and investigating attributes of parks and surrounding areas that regulate cooling effects (Kadaverugu et al., 2021; Ronchi et al., 2020; Zawadzka et al., 2021). Two simulation scenarios were developed: (1) a nominal or ideal condition without influences from surrounding areas, in which cooling effects are solely regulated by the parks' characteristics; and (2) an actual condition incorporating surrounding landscapes' influences, representing the dominant role of neighboring environments in cooling performance. By modeling cooling effects under different scenarios and standardized conditions of background environments, this chapter attempted to minimize uncertainties and biases commonly observed in current studies of urban cooling assessments and to identify key variables supporting evidence-based urban green space planning.

2 Data and methods

2.1 Case studies

This chapter considered the cooling effects of primary public parks along the urban-periphery gradient of the Bangkok metropolis. Five parks were selected based on their usable area (>10 ha) and popularity, of which two parks are located in urban areas and three parks are situated in suburban areas (Fig. 16.1). The most extensive park is Suan Luang Rama IX Park (*hereafter* Rama 9), which is about 80 ha. It was opened in 1987 in the Prawet district to celebrate the 60th birthday of King Rama IX. It is followed by Wachira Benchathat Park, which has 60 ha. This park is in Chatuchak district and is adjacent to Queen Sirikit Park (25.6 ha) and Chatuchak Park (24.8 ha). These three parks together form the great Chatuchak Botanical Garden Complex

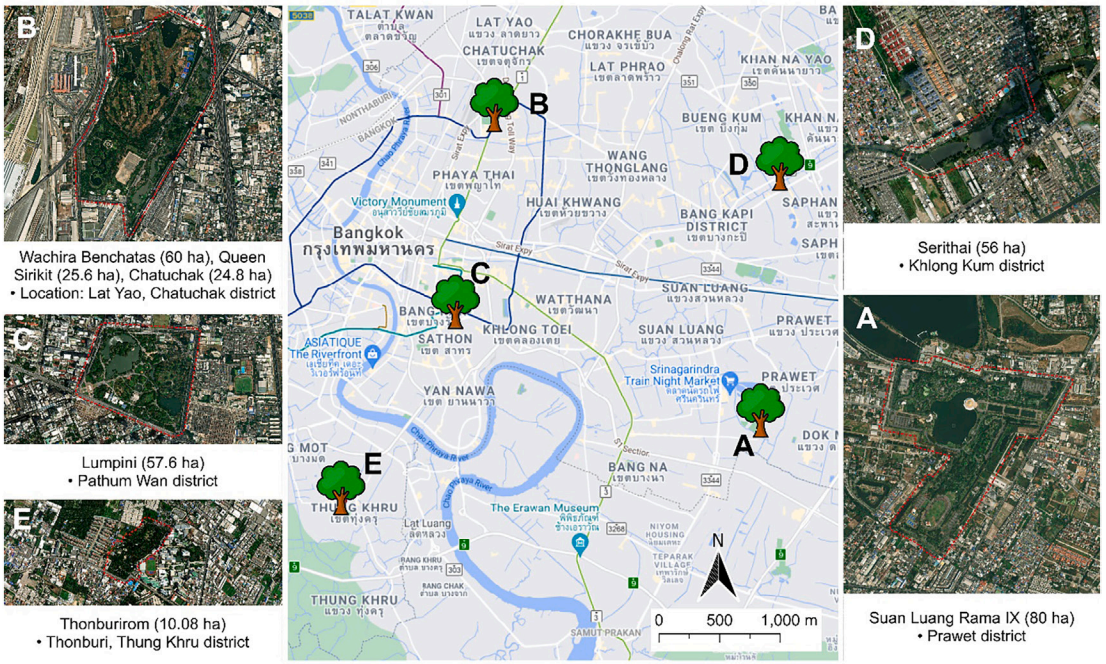


Fig. 16.1 Primary parks along the urban-periurban gradient in the Bangkok metropolis and corresponding scenery from Google Earth images at A—Suan Luang Rama IX, B—Chatuchak Park, C—Lumpini, D—Serithai, and E—Thonburi. Map of urban parks in Bangkok.

(*hereafter* Chatuchak Park), which has over 110 ha and is presently the largest park in Bangkok. One of the oldest parks in Bangkok is Lumpini (57.6 ha) in Pathum Wan district, which was first established in 1925. The park is located in the heart of a cramped city, so it offers an important green asset to its surrounding residents. Serithai Park spreads over 56 ha, which is not much different in usable area compared to Lumpini. This park is located in a periurban region of Khlong Kum district. The dominant scenery is a large lake in the center, serving as natural rainwater storage to prevent flooding during heavy rains. The last considered park is Thonburirom (Thonburi—10.08 ha) in Thung Khru district. It was introduced in 1968 through the conversion of orchards into a public park. As a rare public park in Thonburi, Thonburirom Park is essential to neighboring people as a public space, a place to teach children about nature, and a pollution sink during heavy pollution episodes.

2.2 Remote sensing data

As the spatial extent of individual parks is often small, land use and land cover (LULC) categories of urban parks should be delineated using very-high-resolution (VHR) imagery to

capture spatial patterns and configurations of the park itself at the highest feasible level of detail and to facilitate cross-park comparisons of park design. Yet, commercial VHR imagery could not be acquired for this study due to practical constraints. Fortunately, Google Earth provides free access to VHR imagery, aggregated from commercial and public satellite and aerial sources at different times and spatial scales. Although it lacks the original spatial and spectral information, it is a more cost-effective alternative while still providing sufficiently informative spatial detail. It has been widely applied in numerous urban studies for mapping land use and land cover, assessing green space distribution, monitoring urban growth, and evaluating urban environmental quality (Malarvizhi et al., 2016; Mering et al., 2010). In this study, Google Earth imagery for each park was collected using the SASPlanet tool (v200606), with a pixel size of approximately 30 cm.

Google Earth imagery is indeed proper for detailed LULC mapping at small spatial scales, such as individual parks. However, it shows limitations over extensive regions when the detail of Google Earth images becomes a drawback due to potential noise from building shadows, the colors of different building roof materials, tree canopy structures, and even water surface waves. Therefore, an annual cloud-free composite of Sentinel-2 L2A (10 m) was acquired through Google Earth Engine (GEE) to classify surrounding landscapes in the buffer area around the parks. It was defined as a region covering 2 km from each park since the maximum cooling effect distance (CED) of UGS is frequently <2 km (Aram et al., 2019; Jaganmohan et al., 2016; Nguyen et al., 2024b).

2.3 Land cover classification of parks and surrounding areas

The parks' LULC was classified using Google Earth images and delineated into five LULC categories, including woodland, grassland, soil/pavement, buildings, and water surfaces. Firstly, the acquired Google Earth images were reprojected to the Universal Transverse Mercator (UTM) projection, WGS 84 ellipsoid, zone 47 North (EPSG:32647). These images were then analyzed by object-oriented classification, which is an appropriate classification framework for VHR imagery (Nguyen et al., 2021a). In the object-oriented classification, the images were required to undergo a segmentation procedure, which grouped nearby similar pixels together. The segmented images were then classified using the unsupervised ISODATA (Iterative Self-Organizing Data Analysis) classifier. To cluster pixels into N user-defined groups, the algorithm randomly set cluster centers and assigned pixels to clusters using minimum distance. The clusters were merged or split based on the minimum distance among the cluster centers. The process was repeated until all pixels were precisely separated and the number of clusters reached the user-defined number (N = 30). The classified subclusters were subsequently combined if they represented an identical LULC type in accordance with image visualization and reference data.

LULC in each park's vicinity was delineated using Sentinel-2 multispectral imagery and grouped into major LULC categories such as impervious surfaces, road/pavement, vegetation, water bodies, and bare soil. The multispectral bands were analyzed by integrating principal component analysis (PCA) and the ISODATA unsupervised classifier (Diep et al., 2022). The classified images with separate classes were combined to generate LULC maps. The quality of LULC data for the parks and their neighboring areas achieved high accuracy, which was controlled throughout the classification processes with reference data from different sources, such as image visualization, Google Earth images, Esri land cover data (10 m), and the Regional Land Cover Monitoring System (SERVIR-Mekong).

2.4 Landscape metrics of parks and vicinities

LULC composition and configuration considerably control the cooling effect of UGS since they can amplify or diminish the individual effects of a single UGS through different spatial arrangement patterns with impervious surfaces (Masoudi et al., 2021; McGarigal et al., 2012; Tan et al., 2021). We adopted seven widely used landscape metrics to characterize different aspects of LULC composition and configuration and to investigate their influences on cooling-effect regulation. These indices reflect proportion, patch size, shape, aggregation, and dispersion of LULC categories, including aggregation index (AI), class area (CA), Euclidean nearest-neighbor distance (ENN), largest patch index (LPI), landscape shape index (LSI), patch density (PD), and percentage of landscape (PLAND) (Toutakhane and Mofareh, 2016). The landscape metrics were calculated for the entire park and its vicinity for every 100-meter buffer area from the park's boundary.

2.5 Cooling effect simulation using inVEST urban cooling model

The cooling effects of urban parks were simulated using the InVEST (*Integrated Valuation of Ecosystem Services and Tradeoffs*) urban cooling model (InVEST-UCM, version 3.9.1), which has been developed based on state-of-the-art research on urban heat islands and the cooling effects generated by green infrastructure (Koc et al., 2018; Deilami et al., 2018). The InVEST-UCM model was chosen because it allows straightforward quantification of cooling effects by estimating the heat mitigation index (HMI) and air temperature from LULC, biophysical characteristics, evapotranspiration, and auxiliary parameters at the pixel scale using Equations (1)–(5) (Sharp et al., 2018).

$$CC_i = 0.6 \times Shade + 0.2 \times Albedo + 0.2 \times ETI \tag{1}$$

$$ETI = \frac{K_c \times ET0}{ET_{max}} \tag{2}$$

$$CC_i^{UGS} = \sum_j CC_j \times e^{\left(\frac{-d_{i,j}}{d_{cool}}\right)} \tag{3}$$

$$HMI_i = \begin{cases} CC_i \ \ if\ CC_i \geq CC_i^{UGS} \text{ or } GA_i \leq 2ha \\ CC_i^{UGS}\ if\ CC_i \leq CC_i^{UGS} \text{ or } GA_i \geq 2ha \end{cases} \quad (4)$$

$$T_i^{nomix} = T_{ref} + (1 - HMI_i) \times UHI_{max} \quad (5)$$

LULC is adopted to calculate the cooling capacity (*CC*) for each pixel with contributions from shading (*shade*), evapotranspiration (*ETI*), and albedo (*albedo*) with different ratio weights (Eq. 1) (Kunapo et al., 2018; Zardo et al., 2017). Shading and albedo are LULC-based factors ranging from 0 to 1. A shade of 1 represents full shading by a tree canopy higher than 2 m, and 0 corresponds to non-vegetation LULC types. ETI is a normalized evapotranspiration index, which is calculated from reference evapotranspiration (ET0), the crop coefficient (K_c), and the maximum value of ET0 (ET_{max}; Eq. 2).

The influence of UGS in heat relief is also considered by estimating the cooling capacity provided by UGS (Eq. 3). The cooling capacity of green spaces (CC_i^{UGS}) at a pixel is a cumulative cooling capacity from the adjacent green spaces within the cooling distance (d_{cool}), which is the farthest distance where green spaces still effectively deliver the cooling effect. HMI of a specific pixel is then determined based on Eq. 4. It is equal to the pixel's initial cooling capacity index if its cooling capacity is greater than the cooling capacity of green spaces or the total green spaces area within the cooling distance is smaller than 2 ha. Otherwise, it receives the cooling capacity calculated from green spaces. The InVEST-UCM simulates air temperature based on reference temperature (i.e., the temperature at the rural site, T_{ref}) and maximum urban heat island magnitude (Eq. 5). The simulated air temperature is obtained after applying a Gaussian function with blending distance to simulate the actual air mixing procedures.

The primary inputs for InVEST-UCM are LULC maps adopted from remote sensing data classification. Reference evapotranspiration raster data (version 2) was acquired from the database of the Consultative Group for International Agricultural Research (Zomer and Trabucco, 2019). It is relatively recent, high-resolution potential evapotranspiration data, approximately 1000 m. Yet, the mean value of annual ET0 (ET0 = 1820 mm/year) was applied as a proxy for peer comparison across parks and to ET0 differences due to site location.

The biophysical parameters were summarized in Table 16.1 and proposed by (Hamel et al., 2021), with a wide range of LULC categories. High-density built-up areas were assigned to impervious surfaces outside the parks, while medium-density built-up areas were assigned to impervious surfaces inside the parks. Woodland inside the parks was considered a mixed forest (with mixed vegetation types) and is often under management. Therefore, its crop coefficient is higher than that of shrubland (woodland outside the parks), while the opposite is true for albedo values. It should be noted that both of them were considered UGS with high potential cooling capacity from shading. Water bodies also have a high potential for temperature mitigation via evaporation (Jacobs et al., 2020).

Table 16.1 Biophysical parameters corresponding to each LULC category.

ID	Land cover	Shade	Kc	Albedo	Green space
HB	High-density built-up areas	0	0.179	0.162	0
MB	Medium-density built-up areas	0	0.430	0.208	0
OP	Road/pavement	0	0.516	0.161	0
GR	Grassland	0	0.932	0.193	1
WT	Mixed forest (woodland inside a park)	1	1.004	0.141	1
SH	Shrubland (woodland outside a park, > 2 m)	1	0.968	0.189	1
BS	Bare soil	0	0.613	0.232	0
WA	Water bodies.	0	1.000	0.056	0

Reference temperature and maximum urban heat island (UHI_{max}) magnitude were acquired from the Global Surface Summary of the Day data (GSOD). These are also the proxies used to run InVEST-UCM. More explicitly, the reference temperature was assumed to be the temperature at a station outside Bangkok in Samut Prakan Province in March 2020 (T_{ref} = 29.6°C), when the urban heat island magnitude, measuring the temperature difference between this station and the station inside Bangkok, achieved the maximum value of UHI_{max} = 2.88°C. Furthermore, the cooling distance of green spaces (d_{cool}) was set to be d_{cool} = 100 m since the maximum cooling distance is often around five times the tree height (Kadaverugu et al., 2021; Zardo et al., 2017). Besides, the air blending distance was about 500 m (d_{air} = 500 m) due to the low ventilation rate in urban areas (Bosch et al., 2021; Zawadzka et al., 2021). Model validation was conducted during the trial, and model parameter selection of the cooling distance and the air blending distance was made so that the simulated values were close to the reference values from stations and reanalysis data. It should be noted that this study sets the same neutral conditions (i.e., temperature, UHI, and evapotranspiration) for all parks, and it aims to compare the cooling effects between the parks rather than simulate actual temperatures.

2.6 Assessing controlling factors of heat mitigation and temperature

HMI and Ta of the parks and neighboring areas from the simulation were extracted at every 100 m. This is driven by data characteristics, including a wide range of variables with imbalanced dimensions. Linear regression is inappropriate in this case due to high multicollinearity. Therefore, partial least squares regression (PLSR) was applied to recognize potential predictors for the HMI and Ta dependent variables. In theory, PLSR is also a variable reduction method; however, it involves dependent variables to reflect correlations among predictors and between predictors and dependent variables. The PLSR also respects individual contributions. It is, therefore, widely applied in environmental studies (Cak et al., 2016; Lew et al., 2019; Şuteu

et al., 2021). In addition, the influences of internal and external conditions on the parks' HMI, Ta, and cooling magnitude (i.e., the temperature difference between the park and its vicinity) were investigated using *mixOmics* tools (Rohart et al., 2017). The interrelations were visualized by a correlation circle, while contributions of predictors were detected by the variable importance in projection index (*VIP* > *1*) (Lew et al., 2019; Samad and Bertilsson, 2017).

3 Results

3.1 Land cover of parks and surrounding areas

Image classification from Google Earth images can depict the parks' LULC. These parks are supposed to have a diverse landscape, which incorporates both green and blue spaces in their usable areas in varying ratios (Fig. 16.2). These parks are green assets in the middle of the city, with woodland areas always occupying more than one-third of the total area. In particular, the most prominent is Thonburi, which has a woodland area of up to 60.5% (Table 16.2). If the grassland is also included, the total green space area can reach nearly 80% in Chatuchak and Thonburi parks. Chatuchak and Rama 9 are the parks with the most extensive grassland area, about 30.3% and 23.4%, respectively. Water surface is also an important landscape in these parks as it helps to reduce temperatures by evaporation and

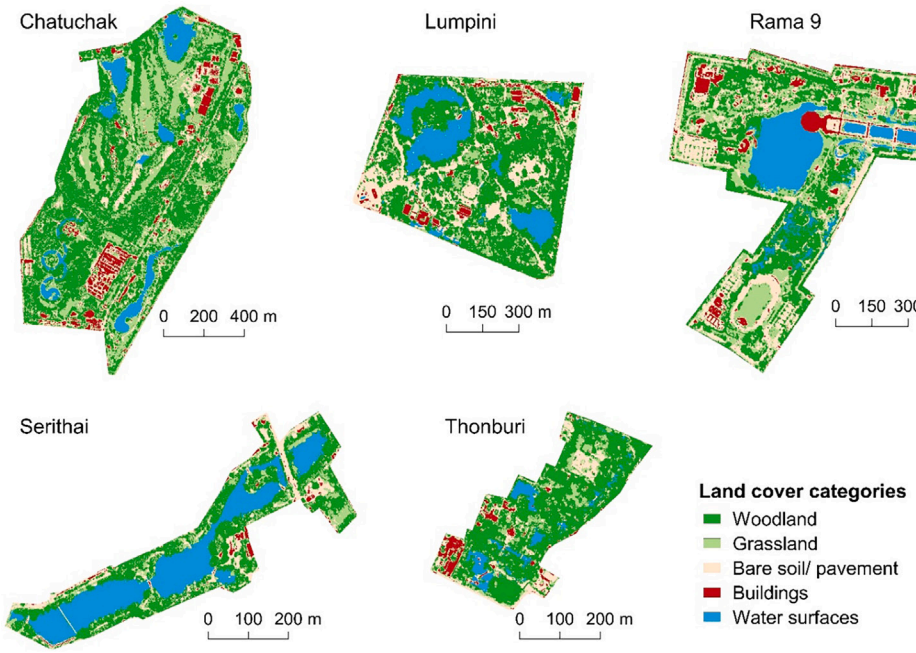


Fig. 16.2 Spatial distribution of LULC delineated from Google Earth images in each park. Land-use and land-cover maps of parks.

facilitates various activities at the parks for urban dwellers. The ratio of water surface area in the parks is very different. For example, it is approximately 7% in Chatuchak and Thonburi, but it is up to 34.9% in Serithai Park.

The characteristics of the parks' surrounding areas are also revealed by Sentinel-2 image interpretation, with the LULC proportions presented in Table 16.2. Specifically, these parks are located in urban and peri-urban areas, where the average built-up area is always higher than 45%. The total impervious surface, including built-up areas and pavements, reaches 68.9% around Chatuchak Park. Based on the proportion of impervious and green surfaces around the parks, Chatuchak is located in the most compact urban area, with the highest impervious surfaces and the lowest green surfaces (27.6%) compared to other parks. In contrast, Rama 9 is located in a more peri-urban area, where nearly 40% of the vicinity is green space. There is also an extensive water area around Rama 9 Park, mainly in the northern area of the park, which is then analyzed for its effect on the park's cooling, as a significant difference compared to the others.

3.2 Simulation of cooling effects

3.2.1 Nominal heat mitigation and temperature

The nominal simulations of parks' heat mitigation were carried out to evaluate the impacts of the parks' characteristics only, excluding external influences outside the parks. Regarding

Table 16.2 Land cover proportion inside the parks and in their surrounding areas. Unit: percent (%).

Inside parks					
Land cover	**Chatuchak**	**Lumphini**	**Rama 9**	**Serithai**	**Thonburi**
Bare soil	8.5	17.6	21.8	10.7	11.9
Built-up	5.0	4.1	6.0	2.0	5.0
Grassland	30.3	12.8	23.4	13.5	15.0
Water surfaces	7.0	13.5	14.2	34.9	7.7
Woodland	49.2	51.9	34.6	38.9	60.5
Neighboring areas					
Land cover	**Chatuchak**	**Lumpini**	**Rama 9**	**Serithai**	**Thonburi**
Bare soil	2.1	2.5	8.6	8.3	3.5
Buildup	56.5	46.0	45.0	47.3	50.8
Road/Pavement	12.4	10.7	2.7	11.7	7.3
Water surfaces	1.5	0.7	3.9	2.4	3.1
Woodland	27.6	40.1	39.9	30.2	35.3

spatial patterns, heat mitigation is proportional to the cooling capacity given by green and blue spaces. It is higher in the center of each park and close to water bodies, where it receives more cumulative effects from adjacent green and blue spaces as cool sources (Fig. 16.3).

Serithai has the most intensive heat mitigation (HMI = 0.867), with about 87% contributed by green and blue spaces. It is followed by Chatuchak and Thonburi, with HMI values of 0.841 and 0.839, respectively. The HMI at Lumpini Park is relatively low compared to other parks (HMI = 0.761). The majority of Rama 9 Park is characterized by low HMI surfaces, constituted by extensive bare land and impervious surfaces. It therefore degrades the park's HMI down to 0.675 (Table 16.3). In this case, the effects of parks were examined separately, without inputs, even positive ones, from the outside environment. These cooling effects are absolutely regarded as background or reference contributions from the parks' characteristics. Therefore, differences in HMI and parks' temperatures originate from the parks' characteristics and patterns.

Air temperature in the parks and HMI are negatively correlated at a high significance level. Air temperature is highest at Rama 9 Park (Ta = 30.50 ± 0.054°C), and it is lowest at Serithai Park (Ta = 29.98 ± 0.032°C). It is followed by Lumpini Park (Ta = 30.28 ± 0.040°C). Thonburi and Chatuchak parks hold rather similar magnitudes of 30.06 ± 0.026°C and 30.05 ± 0.055°C, respectively. The temperatures in Thonburi Park tend to be more homogeneous than other

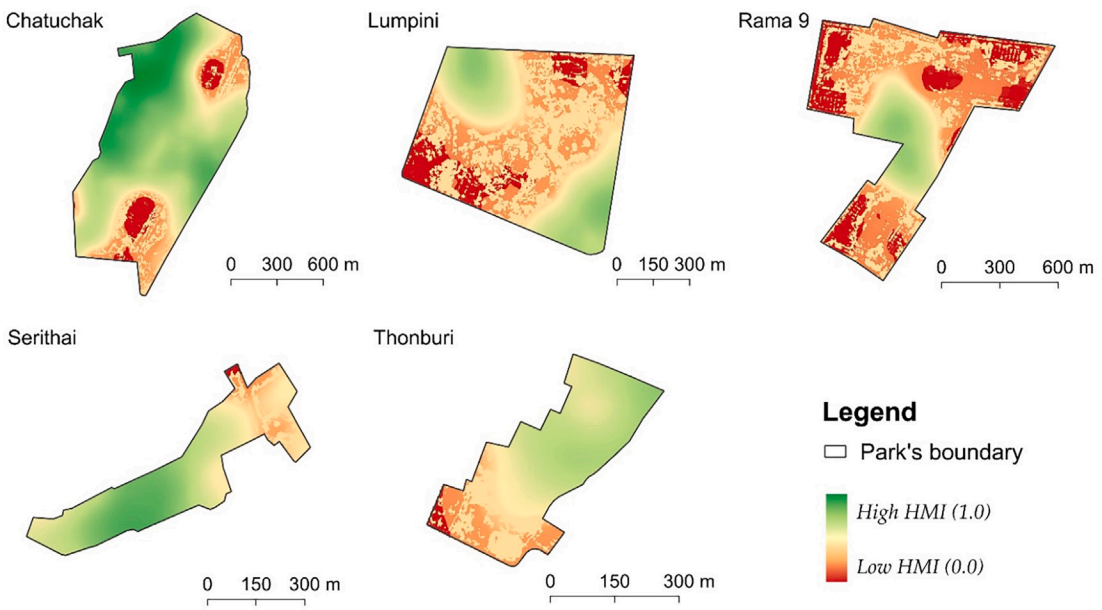


Fig. 16.3 Spatial maps of simulated heat mitigation without the influence of external conditions. Spatial maps of nominal heat mitigation.

Table 16.3 Simulated heat mitigation and temperature from InVEST-UCM.

Heat mitigation index (HMI)	Nominal	Actual	Vicinity
Chatuchak	0.841 ± 0.164	0.741 ± 0.002	0.234 ± 0.291
Lumpini	0.761 ± 0.208	0.705 ± 0.220	0.426 ± 0.366
Rama 9.	0.675 ± 0.259	0.624 ± 0.268	0.448 ± 0.366
Serithai	0.867 ± 0.067	0.572 ± 0.240	0.270 ± 0.314
Thonburi	0.839 ± 0.099	0.677 ± 0.231	0.384 ± 0.366
Air temperature (Ta)			
Chatuchak	30.05 ± 0.055	31.34 ± 0.102	31.52 ± 0.129
Lumpini	30.28 ± 0.040	31.10 ± 0.042	31.17 ± 0.088
Rama 9	30.50 ± 0.054	31.03 ± 0.096	31.12 ± 0.186
Serithai	29.98 ± 0.032	31.54 ± 0.034	31.52 ± 0.096
Thonburi	30.06 ± 0.026	31.35 ± 0.041	31.36 ± 0.162

parks, with the smallest standard deviation value, while the temperature variations within Chatuchak and Rama 9 parks are relatively high, about 0.05°C.

3.2.2 Actual heat mitigation and temperature under environmental interactions

Fig. 16.4 depicts the simulated heat mitigation under the combined effects of interactions between the inside and outside features of the parks. Relative spatial patterns of heat mitigation across the parks remain unchanged regarding cool and heat sources under the actual conditions compared to the nominal conditions. Notwithstanding, significant changes in heat mitigation were found along the park borders and on more sensitive land covers (e.g., water bodies and bare soil). HMI was generally reduced compared to the nominal conditions, while greenery landscapes held a relatively stable HMI.

Quantitatively, the heat mitigation is substantially decreased under combined conditions regarding intensity and order among the parks. Serithai Park drops to the bottom of the list with HMI = 0.572. Rama 9 and Lumpini parks improve their cooling capacity to achieve HMI = 0.624 and HMI = 0.705, respectively. Thonburi is still the second-highest in cooling capacity, although its magnitude is also reduced to just HMI = 0.677. Chatuchak shows the highest cooling capacity, approximately HMI = 0.741. Every park encounters HMI degradation to different extents, from 7.0% up to 34%. Lumpini and Rama 9 parks are supposed to be relatively stable, with a rate of change of about 7% compared to the initial values. Whereas this rate is higher in Thonburi Park (19.3%), it reaches the highest rate in Serithai Park (33.9%). Heat mitigation and air temperature at the park, in this case, still exist in close connection. It is, however, a low relationship ($r = -0.28$). In particular, it is about 31.54 ± 0.034°C in Serithai Park, then followed by Thonburi and Chatuchak parks at approximately 31.34–31.35°C. The temperature in Lumpini Park is cooler than the other parks, with 31.10 ± 0.042°C. Among

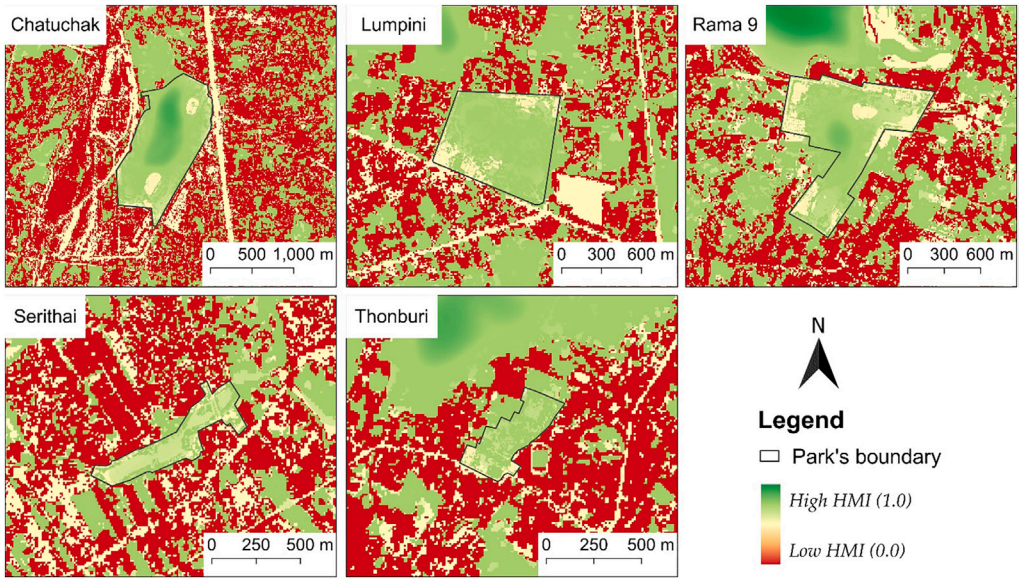


Fig. 16.4 Spatial distribution of actual heat mitigation in parks and surrounding areas. Spatial maps of actual heat mitigation.

the parks, Rama 9 has the most intensive temperature regulation, and its temperature is about 31.03 ± 0.10°C.

3.3 Relationships between landscape patterns and cooling effects

3.3.1 Nominal heat mitigation and park's temperature

Firstly, the park's land-cover-related elements controlling heat mitigation and air temperature under nominal conditions were examined (Fig. 16.5). The results revealed that HMI and Ta can be explained by the first component (Component 1, about 69.2% of the variance), reaching 98.3% with the contribution from the first two components (Component 1 and Component 2). Under nominal conditions, every landscape regulates the cooling effect via a few certain aspects of landscape characteristics, with the exception of LPI (Fig. 16.5B). The impact trend and magnitude of each element on HMI and Ta are shown in the correlation circle of Fig. 16.5A. HMI is positively stimulated by high PD in the decreasing order of medium built-up > woodlands > grasslands. In contrast, HMI is restrained by several elements. HMI and Ta, however, are negatively correlated with these elements, meaning that these elements will improve the cooling effect. These elements include ENN of woodlands and grasslands, AI of grasslands, medium built-up, and woodlands, PD of grasslands and woodlands, CA and LSI of water bodies, and PLAND of medium built-up. Among them, the distance between green patches is the most substantial contributor to the increased cooling effect of the parks. Aggregating landscapes and water-related metrics contribute less to the cooling effect than other elements.

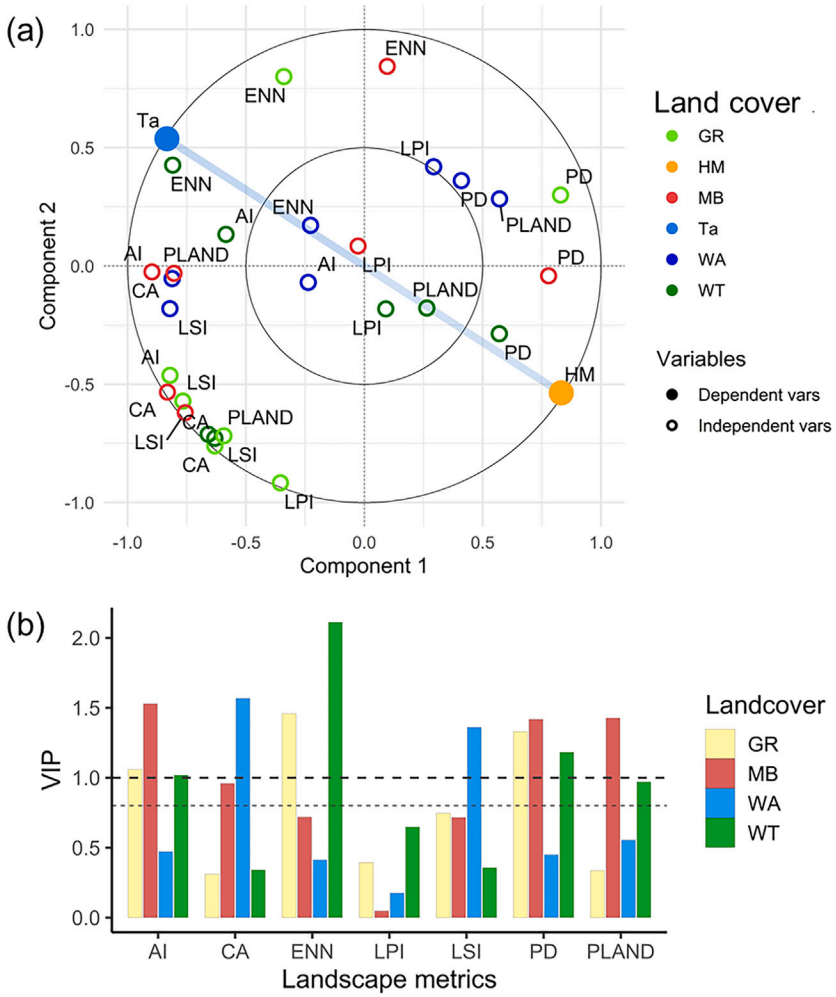


Fig. 16.5 Primary results from PLSR reveal (a) correlation circle between internal predictors and dependent variables, and (b) variable selection for Component 1 based on VIP for HMI and park temperature under nominal conditions. Results from the PLSR analysis are for nominal conditions.

3.3.2 Actual heat mitigation and temperature under combined conditions

Fig. 16.6 illustrates the intercorrelation between internal and external variables and inside and outside cooling effects from the PLSR analyses.

3.3.3 Park's impact on outside environments

Under the influence of combined conditions, the parks' HMI showed a weak connection with their relative temperature, and no direct link was found between the parks' HMI and surrounding temperature (i.e., they are in orthogonal directions). However, it does not mean that the park

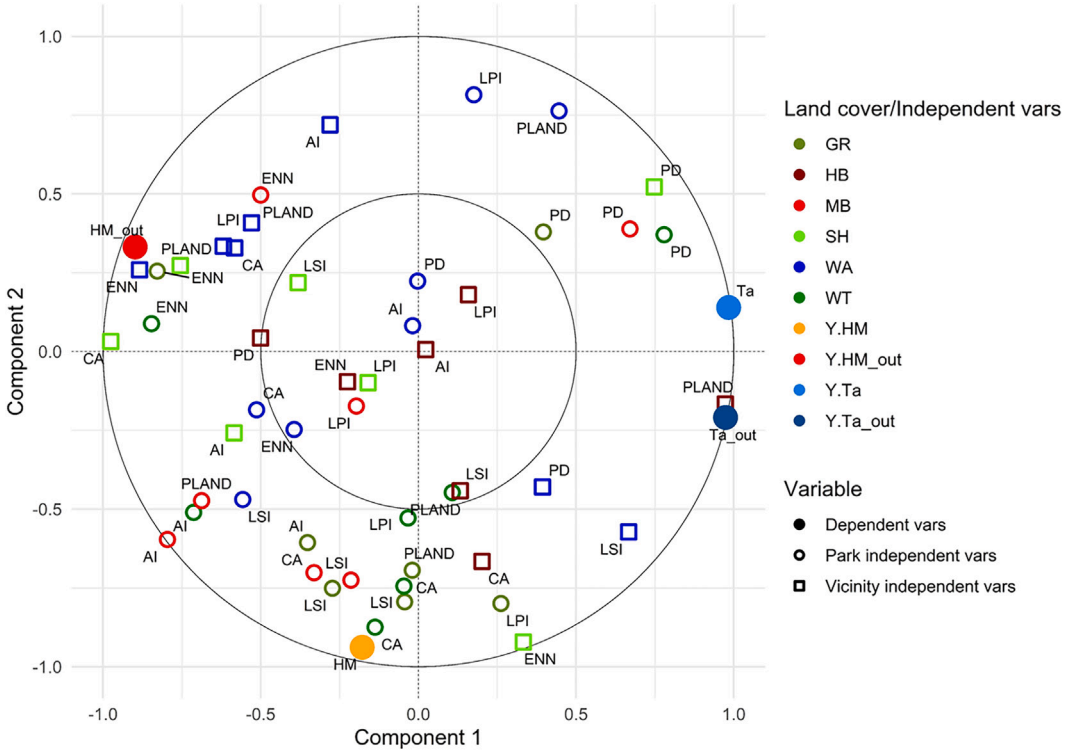


Fig. 16.6 General correlation circle between internal and external predictors and the dependent variables of the park and surrounding areas. Results from the PLSR analysis for actual conditions.

has no impact on the surrounding environments. It is apparently evident that external elements dominate the surrounding temperature through the overall HMI values ($r = -0.96$, $p < 0.01$). It was found that the park's patterns also indirectly control the surrounding temperature as latent factors. The internal conditions can explain 84.5% of the external temperature with only Component 1. Among the elements, the adjustments of the nearest distance (ENN) between the features (e.g., grassland, woodland, and impervious surfaces) and increased aggregation for woodland (AI) will greatly improve the park's cooling effect to deliver cool air flows outward efficiently.

3.3.4 External conditions affecting the parks

The potential feedback from parks when placed in different backgrounds was investigated. It was revealed that external environments also adjust the park's HMI (71.6%, Component 1) and temperature (82.3%, Component 1). The park's HMI is stimulated when the park is placed in a region with highly aggregated shrublands (AI) at shorter distances among green patches. The appearance of water surfaces with more complex shapes also assists the park's HMI.

The same holds for the park's temperature. It is alleviated mainly by water features through increasing patch size (LPI) and the improvement of the area (CA) and proportion (PLAND) of shrublands. It should also be noted that an increase in the built-up proportion significantly raises the park's temperature.

3.3.5 Combined conditions affecting cooling magnitude

The elements affecting cooling magnitude, i.e., the temperature difference inside versus outside the parks, were also investigated. The PLSR was convinced that controlling for internal and external variables could explain up to 95.8% of the temperature differences (Component 1). The external environments improve cooling magnitude when the distance between green patches (ENN) narrows. A dense concentration (AI) with a high area (CA) of impervious surfaces also amplifies these differences. However, it has a negative effect when considering its nature, because this attribute will heat up the background temperatures. Most of the contributions are from internal elements from diverse landscapes. Among them, the most significant contributors to cooling magnitude are ENN of impervious surfaces (*negative*), grasslands (LPI > PLAND > AI > CA > LSI), water bodies (LSI > CA), and woodlands (LSI > CA).

4 Discussions

4.1 Interrelationship between landscape configurations

It is apparent within a certain area that a landscape's proportion and distributive patterns adjust the characteristics of other landscapes, especially for the adjacent features. The landscape metrics are closely related to each other both inside and outside the parks (Figs. 16.5 and 16.6). Some typically positive connections can be found for CA–PLAND–LPI, implying an increase in class total area and its proportion will amplify the patch size. Besides, LSI–PD means an increase in the number of individual patches linked to the shape complexity of these patches. In contrast, improving patches' aggregation decreases shape complexity and patch density. Whereas the quantitative richness of class area declines the nearest distance between the patches, it causes patch size, shape complexity, and patch density growth. The lawns are often planted between the patches of woodlands and shrublands, so these green space types are also closely related. These interrelations can facilitate park redesign plans when some landscape characteristics need improvement. In this case, the planners can simplify them by adjusting a core aspect instead of considering all elements of landscape configurations. Supposedly, if we would like to improve the patch size, patch density, and shape complexity of woodlands, we can plant more trees on grassland to shorten the nearest distance among the patches of trees. Yet, it boosts the multicollinearity in regression models and induces overfitted models. Hence, it should be decided to study the prominent landscapes and metrics of interest rather than considering them all generally.

4.2 Implications for an "ideal park" design

The cooling mechanisms of urban parks are complicated due to both the park's structure itself and the background environments. The nominal assessment of HMI and Ta for the park constrains the influences of surrounding environments on the park's cooling performance. It reflects the background cooling capacity generated by the parks and reveals a prototype park that maximizes cooling effects. Without stimulation from external conditions, the parks' HMI and their Ta are straightforwardly associated. Therefore, the cooler park with a higher HMI can be considered a prototype park. A group of three parks (i.e., Serithai, Chatuchak, and Thonburi) could be considered as prototype parks. Regarding landscape proportion, there are two potential options to optimize the cooling effect: (1) to be dominated by large water bodies (Serithai) and (2) to have accumulative green spaces above 70% (including lawns and woodlands).

Green parks and wetlands are essential in adaptation and resilience strategies to climate changes and urbanization when cities are gradually crowded, and microclimates with heatwaves are increasingly harsh. Vegetation supplies diverse benefits, e.g., air purification, temperature regulation, and aesthetic values (Nguyen and Chidthaisong, 2023). Besides, water surfaces and wetlands are appreciated because they have a high cooling capacity through evapotranspiration, which increases air humidity (Amani-Beni et al., 2018; Kuşçu Şimşek and Ödül, 2018; Xue et al., 2019). Wetlands also contribute to biodiversity in cities through their aquatic ecosystems. It also diversifies the landscapes and activities in urban parks. Understanding the importance of water surfaces and wetlands, most parks in Bangkok retain water surfaces at a rate from 7% (Chatuchak) up to 34.6% (Serithai). The average ratio is 10–15%, while the majority is still the vegetated surfaces, e.g., lawns, flowers, shrubs, and tall trees. However, the landscape configuration has a more significant influence on the cooling performance than proportion. It is straightforward that increasing the water surface area with a simple lake shape (e.g., circle/rectangle, see example in (Campbell et al., 2015)) will increase the cooling performance. In contrast, controlling woodlands and grasslands is relatively complicated through a few parameters, such as shortening the distance between individual tree patches, which will significantly improve the park's HMI and Ta. On the other hand, advances in the shortest distance and aggregation of grassland will diminish the cooling effect, implying grass patches should be distributed far apart or between patches of trees. Furthermore, the cooling magnitude is mainly contributed by the park characteristics, which is higher than 23% compared to external conditions. It is stimulated by increasing the total area of green spaces and the shape complexity of landscapes, as well as maintaining the patch size of green spaces.

These research findings revealed that most of the landscape metrics were from grasslands and woodlands rather than a particular landscape. It is consistent with previous studies that combining landscapes strengthens heat reduction rather than individual effects. Combinations

of trees–grasslands and water–trees are the most efficient among natural pairs (Xu et al., 2017). Fortunately, all the studied parks applied these combinations to varying degrees. Nevertheless, the proportion of water bodies versus green spaces should be considered carefully. Green spaces should still be the essential object because a high ratio of water surfaces can reduce the cooling magnitude of a park. Plus, water surfaces only have a favorable cooling effect when unpolluted because pollutants and matter in water encourage heat absorption. Water surfaces also slow down the heat release at night. Yet, water surface cooling capacity is enhanced during hot daytime because evapotranspiration is stimulated by high temperatures and wind (Nguyen et al., 2024b; Wang et al., 2018). Meanwhile, the cooling effect of green spaces is relatively consistent over time by providing shade, humidification, and heat absorption. Therefore, ratios of vegetated and water surfaces (or green-blue spaces) should be carefully cogitated to diversify landscapes and optimize the cooling effect throughout the time.

4.3 Influences of external environments

It is widely acknowledged that UGS and urban parks improve urban environments. However, vegetation within hostile urban matrices hinders growth, phenology, and productivity (Liang and Wang, 2020). It also limits the effective distribution of cooling capacity to the surrounding environments. This research showcased the important control of external conditions on the parks' heat mitigation, temperatures, and cooling magnitude. The influences of the parks' vicinities align with previous studies (Blachowski and Hajnrych, 2021; Cheng et al., 2015; Qiu and Jia, 2020). The existence of water bodies and green spaces crucially facilitates the enhancement of the parks' cooling effects. It will be optimized when these cool surfaces increase in their proportion and agglomeration.

In contrast, it is apparent that the escalation of impervious surfaces around the park significantly diminishes the park's cooling effects. To some extent, this will put pressure on the vegetation's health and cause a reduction in the inherent cooling efficiency of parks. In addition to considering park size and landscape configurations, park location, the distance between parks and large green spaces, and the surrounding environments deserve consideration. This will benefit urban residents by increasing opportunities to engage in activities in green spaces, reducing possible pressures on parks, optimizing cooling efficiency for cities, and increasing biodiversity in parks. The current research continues to provide evidence of the need to ensure a minimum distance between urban green areas. It indicates benefits from a biodiversity perspective (Chaiyarat et al., 2019) while this study adds a stance on the accumulative cooling effect.

4.4 Limitations and future work

This chapter attempted to address the limitations in previous studies, which assessed the park's cooling effect using HMI and Ta instead of LST (Cheng et al., 2015; Qiu and Jia, 2020).

Notwithstanding, the InVEST-UCM can involve LULC characteristics in Ta estimation, thereby reflecting the fundamental differences between the parks in terms of landscape composition and configuration. This model still has some limitations regarding data and parameters that might cause uncertainties and biases. Evapotranspiration data are frequent at a coarse scale; they are therefore difficult to apply at local scales. The parameters related to green space cooling distance and air mixing distance are highly varying among cities with different climates, tree species, and even urban morphology, thereby requiring particular empirical studies to identify them for more precise studies.

Yet this study also suggests future research directions to better understand urban cooling mechanisms. Temporal changes in the cooling effect should be studied to detect differences between a large water park and a pure green park throughout the day and across seasons. Therefore, we could have more detailed recommendations on the involvement of water bodies in the urban park to maximize the park's cooling effect. Furthermore, tree species in each park are supposed to disparately affect cooling capacity in spatial and temporal aspects. For instance, the regulation capacity of deciduous species is weakened during the leaf-change season. Although the differences due to species combinations have not yet been studied, based on plant physiology, evergreen species should be considered an essential vegetation type in parks in tropical countries. Nonetheless, further detailed studies on tree species should be conducted to optimize air regulation while respecting native plant species.

5 Conclusion

This chapter applied the InVEST-UCM to estimate HMI and Ta at the five major parks in the Bangkok metropolis and evaluate the cooling effects. It revealed that Serithai, Chatuchak, and Thonburi are the parks with the highest HMI and can dramatically regulate temperatures compared to the others. The cooling effects of a certain park are mainly stimulated by woodlands, grasslands, and water bodies, and by increasing water surface area and shape complexity. It can also be improved by enhancing the agglomeration and shape complexity of woodland patches that interact with grasslands. Meanwhile, the surrounding areas have an important influence on the park's temperatures and its cooling magnitude. A more compact neighboring area will put more pressure on urban parks, diminish heat mitigation capacity, and elevate the ambient temperatures. On the other hand, the synergy of external blue-green spaces can amplify the cooling magnitude, especially when they are more compact and clustered. The research findings consolidate the cooling effects provided by urban parks in tropical monsoon regions with complicated connections both inside and outside the parks, thereby enabling appropriate spatial plans to renovate current parks and establish new parks to cool down the city effectively.

Acknowledgments

This work was financially supported by the Petchra Pra Jom Klao Doctoral Scholarship (09/2562) of King Mongkut's University of Technology Thonburi (KMUTT). We thank Sanwit Iabchoon for valuable comments on this chapter.

References

Abrar, R., Sarkar, S.K., Nishtha, K.T., Talukdar, S., Shahfahad, A.R., Islam, A.R.M.T., Mosavi, A., 2022. Assessing the spatial mapping of heat vulnerability under Urban Heat Island (UHI) effect in the Dhaka Metropolitan Area. Sustainability. 20711050. 14 (9). Available from: https://www.mdpi.com/2071-1050/14/9/4945/pdf. doi:10.3390/su14094945.

Amani-Beni, M., Zhang, B., Xie, G.D., Xu, J., 2018. Impact of urban park's tree, grass and waterbody on microclimate in hot summer days: a case study of Olympic Park in Beijing, China. Urban For. Urban Green. 16108167. 32, 1–6. Available from: http://www.elsevier.com/wps/find/journaldescription.cws_home/701803/description#description. doi:10.1016/j.ufug.2018.03.016.

Aram, F., García, E.H., Solgi, E., Mansournia, S., 2019. Urban green space cooling effect in cities. Heliyon. 24058440. 5 (4), e01339. doi:10.1016/j.heliyon.2019.e01339.

Blachowski, J., Hajnrych, M., 2021. Assessing the cooling effect of four urban parks of different sizes in a temperate continental climate zone: Wroclaw (Poland). Forests. 1999-4907. 12 (8), 1136. doi:10.3390/f12081136.

Bosch, M., Locatelli, M., Hamel, P., Remme, R.P., Chenal, J., Joost, S., 2021. A spatially explicit approach to simulate urban heat mitigation with InVEST (v3.8.0). Geosci. Model Dev. 19919603. 14 (6), 3521–3537. Available from: http://www.geosci-model-dev.net/volumes_and_issues.html. doi:10.5194/gmd-14-3521-2021.

Cak, A.D., Moran, E.F., Figueiredo, R.D.O., Lu, D., Li, G., Hetrick, S., 2016. Urbanization and small household agricultural land use choices in the Brazilian Amazon and the role for the water chemistry of small streams. J. Land Use Sci. 17474248. 11 (2), 203–221. Available from: http://www.tandf.co.uk/journals/titles/1747423x.asp. doi:10.1080/1747423X.2015.1047909.

Campbell, L.P., Finley, A.O., Benbow, M.E., Gronseth, J., Small, P., Johnson, R.C., Sopoh, G.E., Merritt, R.M., Williamson, H., Qi, J., 2015. Spatial analysis of anthropogenic landscape disturbance and Buruli Ulcer disease in Benin. PLoS Negl. Trop. Dis. 19352735. 9 (10). Available from: http://www.plosntds.org/index.php. doi:10.1371/journal.pntd.0004123.

Chaiyarat, R., Wutthithai, O., Punwong, P., 2019. Wut Taksintam, relationships between urban parks and bird diversity in the Bangkok metropolitan area, Thailand. Urban Ecosyst. 1083-8155. 22 (1), 201–212. doi:10.1007/s11252-018-0807-1.

Chaston, T.B., Broome, R.A., Cooper, N., Duck, G., Geromboux, C., Guo, Y., Ji, F., Perkins-Kirkpatrick, S., Zhang, Y., Dissanayake, G.S., Morgan, G.G., Hanigan, I.C., 2022. Mortality burden of heatwaves in Sydney, Australia is exacerbated by the urban heat island and climate change: can tree cover help mitigate the health impacts? Atmosphere. 20734433. 13 (5). Available from: https://www.mdpi.com/2073-4433/13/5/714/pdf?version=1651310355. doi:10.3390/atmos13050714.

Cheng, X., Wei, B., Chen, G., Li, J., 2015. Conghe song, influence of park size and its surrounding urban landscape patterns on the park cooling effect. J. Urban Plan. Dev. 0733-9488. 141 (3). doi:10.1061/(asce)up.1943-5444.0000256.

Chung, J., Kim, J., Sung, K., 2024. Analysis of heat mitigation capacity in a coastal city using InVEST urban cooling model. Sustain. Cities Soc. 22106707. 113, 105669. doi:10.1016/j.scs.2024.105669.

Deilami, K., Kamruzzaman, M., Liu, Y., 2018. Urban heat island effect: a systematic review of spatio-temporal factors, data, methods, and mitigation measures. Int. J. Appl. Earth Obs. Geoinf. 15698432. 67, 30–42. doi:10.1016/j.jag.2017.12.009.

Diep, N.T.H., Trong Nguyen, C., Kieu Diem, P., Xuan Hoang, N., Al Kafy, A., 2022. Assessment on controlling factors of urbanization possibility in a newly developing city of the Vietnamese Mekong delta using logistic regression analysis. Phys. Chem. Earth. 14747065. 126. doi:10.1016/j.pce.2021.103065.

Estoque, R.C., Murayama, Y., 2017. Monitoring surface urban heat island formation in a tropical mountain city using Landsat data (1987–2015). ISPRS J. Photogramm. Remote Sens. 09242716. 133, 18–29. Available from: www.elsevier.com/inca/publications/store/5/0/3/3/4/0. doi:10.1016/j.isprsjprs.2017.09.008.

Estoque, R.C., Murayama, Y., Myint, S.W., 2017. Effects of landscape composition and pattern on land surface temperature: an urban heat island study in the megacities of Southeast Asia. Sci. Total Environ. 18791026. 577, 349–359. Available from: www.elsevier.com/locate/scitotenv. doi:10.1016/j.scitotenv.2016.10.195.

Hamel, P., Guerry, A.D., Polasky, S., Han, B., Douglass, J.A., Hamann, M., Janke, B., Kuiper, J.J., Levrel, H., Liu, H., Lonsdorf, E., McDonald, R.I., Nootenboom, C., Ouyang, Z., Remme, R.P., Sharp, R.P., Tardieu, L., Viguié, V., Xu, D., Zheng, H., Daily, G.C., 2021. Mapping the benefits of nature in cities with the InVEST software. Npj Urban Sustain. 2661-8001. 1 (1). doi:10.1038/s42949-021-00027-9.

Hu, Y., Wang, C., Li, J., 2023. Assessment of heat mitigation services provided by blue and green spaces: an application of the InVEST urban cooling model with scenario analysis in Wuhan, China. Land. 2073-445X. 12 (5), 963. doi:10.3390/land12050963.

Jacobs, C., Klok, L., Bruse, M., Cortesão, J., Lenzholzer, S., Kluck, J., 2020. Are urban water bodies really cooling? Urban Clim. 22120955. 32, 100607. doi:10.1016/j.uclim.2020.100607.

Jaganmohan, M., Knapp, S., Buchmann, C.M., Schwarz, N., 2016. The bigger, the better? The influence of urban green space design on cooling effects for residential areas. J. Environ. Qual. 15372537. 45 (1), 134–145. Available from: https://dl.sciencesocieties.org/publications/jeq/pdfs/45/1/134. doi:10.2134/jeq2015.01.0062.

Kadaverugu, R., Gurav, C., Rai, A., Sharma, A., Matli, C., Biniwale, R., 2021. Quantification of heat mitigation by urban green spaces using InVEST model—a scenario analysis of Nagpur City, India. Arab. J. Geosci. 1866-7511. 14 (2). doi:10.1007/s12517-020-06380-w.

Khamchiangta, D., Dhakal, S., 2019. Physical and non-physical factors driving urban heat island: case of Bangkok Metropolitan Administration, Thailand. J. Environ. Manag. 03014797. 248, 109285. doi:10.1016/j.jenvman.2019.109285.

Khamchiangta, D., Dhakal, S., 2020. Time series analysis of land use and land cover changes related to urban heat island intensity: case of Bangkok Metropolitan Area in Thailand. J. Urban Manag. 22265856. 9 (4), 383–395. doi:10.1016/j.jum.2020.09.001.

Koc, C.B., Osmond, P., Peters, A., 2018. Evaluating the cooling effects of green infrastructure: a systematic review of methods, indicators and data sources. Sol. Energy. 0038092X. 166, 486–508. doi:10.1016/j.solener.2018.03.008.

Kraemer, R., Kabisch, N., 2022. Parks under stress: air temperature regulation of urban green spaces under conditions of drought and summer heat. Front. Environ. Sci. 2296-665X. 10. doi:10.3389/fenvs.2022.849965.

Kunapo, J., Fletcher, T.D., Ladson, A.R., Cunningham, L., Burns, M.J., 2018. A spatially explicit framework for climate adaptation. Urban Water J. 17449006. 15 (2), 159–166. Available from: http://www.tandf.co.uk/journals/titles/1573062X.asp. doi:10.1080/1573062X.2018.1424216.

Kuşçu Şimşek, Ç., Ödül, H., 2018. Investigation of the effects of wetlands on micro-climate. Appl. Geogr. 01436228. 97, 48–60. doi:10.1016/j.apgeog.2018.05.018.

Lew, S., Glińska-Lewczuk, K., Lew, M., Ban, S., 2019. The effects of environmental parameters on the microbial activity in peat-bog lakes. Plos One. 1932-6203. 14 (10), e0224441. doi:10.1371/journal.pone.0224441.

Liang, S., Wang, J., 2020. Urbanization: monitoring and impact assessment. Adv. Remote Sens. 833–870. doi:10.1016/B978-0-12-815826-5.00023-4.

Malarvizhi, K., Vasantha Kumar, S., Porchelvan, P., 2016. Use of high resolution google earth satellite imagery in landuse map preparation for urban related applications. Procedia Technol. 22120173. 24, 1835–1842. doi:10.1016/j.protcy.2016.05.231.

Masoudi, M., Tan, P.Y., Fadaei, M., 2021. The effects of land use on spatial pattern of urban green spaces and their cooling ability. Urban Clim. 22120955. 35, 100743. doi:10.1016/j.uclim.2020.100743.

McGarigal, K., Cushman, S.A., Ene, E., 2012. FRAGSTATS v4: spatial pattern analysis program for categorical and continuous maps.

Mering, C., Baro, J., Upegui, E., 2010. Retrieving urban areas on Google Earth images: application to towns of West Africa. Int. J. Remote Sens. 0143-1161. 31 (22), 5867–5877. doi:10.1080/01431161.2010.512311.

Nguyen, C.T., Amnat, C., Rungnapa, K., Wijitbusaba, M., 2023. Urban thermal environment under urban expansion and climate change: a regional perspective from southeast Asian big cities. Clim. Change Cooling Cities 151–167. doi:10.1007/978-981-99-3675-5_9.

Nguyen, C.T., Chidthaisong, A., 2023. Ecosystem services provided by urban green spaces in Bangkok Metropolis: public awareness and planning implications. Urban Ecosyst. 27. doi:10.1007/s11252-023-01482-1

Nguyen, C.T., Chidthaisong, A., Kaewthongrach, R., 2024b. Assessment of cooling effect by urban park using a multi-data source approachassessment of cooling effect by Urban Park using a multi-data source approach. Proceedings of the 8th International Conference on Sustainable Urban Development. ICSUD 2022. Advances in 21st Century Human Settlements. 9789819980031. 129–144, Available from: http://dx.doi.org/10.1007/978-981-99-8003-1_9. doi: 10.1007/978-981-99-8003-1_9.

Nguyen, C.T., Chidthaisong, A., Limsakul, A., Varnakovida, P., Ekkawatpanit, C., Diem, P.K., Diep, N.T.H., 2022. How do disparate urbanization and climate change imprint on urban thermal variations? A comparison between two dynamic cities in Southeast Asia. Sustain. Cities Soc. 22106707. 82. Available from: http://www.elsevier.com/wps/find/journaldescription.cws_home/724360/description#description. doi:10.1016/j.scs.2022.103882.

Nguyen, C.T., Diep, N.T.H., Iabchoon, S., 2021a. Direction of urban expansion in the Bangkok Metropolitan Area, Thailand under the impacts of a national strategy. J. Earth Sci. 26159783. 43 (3), 380–398. Available from: https://vjs.ac.vn/index.php/jse/article/view/16313/103810384717. doi:10.15625/2615-9783/16313.

Nguyen, C.T., Nguyen, D.T.H., Phan, D.K., 2021b. Factors affecting urban electricity consumption: a case study in the Bangkok Metropolitan Area using an integrated approach of earth observation data and data analysis. Environ. Sci. Pollut. Res. 16147499. 28 (10), 12056–12066. Available from: https://link.springer.com/journal/11356. doi:10.1007/s11356-020-09157-6.

Nguyen, C.T., Nguyen, H., Sakti, A.D., 2024a. Seasonal characteristics of outdoor thermal comfort and residential electricity consumption: a Snapshot in Bangkok Metropolitan Area. Remote Sens. Appl. Soc. Environ. 33. doi:10.1016/j.rsase.2023.101106

Nguyen, C.T., Noszczyk, T., Iabchoon, S., 2025. Soil Textures and Urban Heat Cooling Planning Strategies Remote Sensing for Geophysicists. CRC Press, Czech Republic, pp. 472–484. Available from https://www.taylorfrancis.com/books/edit/10.1201/9781003485278. doi:10.1201/9781003485278-40.

Piracha, A., Chaudhary, M.T., 2022. Urban air pollution, urban heat island and human health: a review of the literature. Sustainability. 2071-1050. 14 (15), 9234. doi:10.3390/su14159234.

Qiu, K., Jia, B., 2020. The roles of landscape both inside the park and the surroundings in park cooling effect. Sustain. Cities Soc. 22106707. 52, 101864. doi:10.1016/j.scs.2019.101864.

Räsänen, A., Heikkinen, K., Piila, N., Juhola, S., 2019. Zoning and weighting in urban heat island vulnerability and risk mapping in Helsinki, Finland. Reg. Environ. Change. 1436-3798. 19 (5), 1481–1493. doi:10.1007/s10113-019-01491-x.

Rohart, F., Gautier, B., Singh, A., Lê Cao, K.A., 2017. mixOmics: an R package for 'omics feature selection and multiple data integration. PLoS Comput. Biol. 15537358. 13 (11). Available from: http://www.ploscompbiol.org/article/browseVolume.action?field=volume. doi:10.1371/journal.pcbi.1005752.

Ronchi, S., Salata, S., Arcidiacono, A., 2020. Which urban design parameters provide climate-proof cities? An application of the Urban Cooling InVEST Model in the city of Milan comparing historical planning morphologies. Sustain. Cities Soc. 22106707. 63, 102459. doi:10.1016/j.scs.2020.102459.

Samad, M.S., Bertilsson, S., 2017. Seasonal variation in abundance and diversity of bacterial methanotrophs in five temperate lakes. Front. Microbiol. 1664302X. 8. Available from: http://journal.frontiersin.org/article/10.3389/fmicb.2017.00142/full. doi:10.3389/fmicb.2017.00142.

Sharp, R., Tallis, H.T., Ricketts, T., Guerry, A.D., Wood, S.A., Chaplin-Kramer, R., Nelson, E., Ennaanay, D., Wolny, S., Olwero, N., Vigerstol, K., Pennington, D., Mendoza, G., Aukema, J., Foster, J., Forrest, J., Cameron, D., Arkema, K., Lonsdorf, E., Kennedy, C., Verutes, G., Kim, C.K., Guannel, G., Papenfus, M., Toft, J., Marsik, M., Bernhardt, J., Griffin, R., Glowinski, K., Chaumont, N., Perelman, A., Lacayo, M., Mandle, L., Hamel, P., Vogl, A.L., Rogers, L., Bierbower, W., Denu, D. & Douglass, J. 2018. InVEST 3.6.0 User's Guide. Collaborative Publication by The Natural Capital Project, Stanford University, the University of Minnesota, The Nature Conservancy, and the World Wildlife Fund. Stanford University, Stanford. Available from: https://naturalcapitalproject.stanford.edu/software/invest.

Singh, N., Singh, S., Mall, R.K., 2020. Urban ecology and human health: implications of urban heat island, air pollution and climate change nexus urban ecology: emerging patterns and social-ecological systems. Elsevier, India, pp. 317–334. Available from https://www.elsevier.com/books/urban-ecology/verma/978-0-12-820730-7. doi:10.1016/B978-0-12-820730-7.00017-3.

Son, N.T., Chen, C.F., Chen, C.R., Thanh, B.X., Vuong, T.H., 2017. Assessment of urbanization and urban heat islands in Ho Chi Minh City, Vietnam using Landsat data. Sustain. Cities Soc. 22106707. 30, 150–161. Available from: http://www.elsevier.com/wps/find/journaldescription.cws_home/724360/description#description. doi:10.1016/j.scs.2017.01.009.

Şuteu, A.M., Momeu, L., Battes, K.P., Baricz, A., Cristea, A., Bulzu, P.A., Buda, D.M., Banciu, H.L., Cîmpean, M., 2021. Diversity and distribution of phototrophic primary producers in saline lakes from Transylvania, Romania. Plant Syst. Evol. 16156110. 307 (1). Available from: www.springer.com/journal/606. doi:10.1007/s00606-020-01733-0.

Tan, X., Sun, X., Huang, C., Yuan, Y., Hou, D., 2021. Comparison of cooling effect between green space and water body. Sustain. Cities Soc. 22106707. 67. Available from: http://www.elsevier.com/wps/find/journaldescription.cws_home/724360/description#description. doi:10.1016/j.scs.2021.102711.

Toutakhane, A.M., Mofareh, M., 2016. Investigation and evaluation of spatial patterns in tabriz parks using landscape metrics. J. Urban Environ. Eng. 19823932. 10 (2), 263–269. Available from: http://periodicos.ufpb.br/ojs2/index.php/juee/article/download/30480/pdf. doi:10.4090/juee.2016.v10n2.263269.

Vujovic, S., Haddad, B., Karaky, H., Sebaibi, N., Boutouil, M., 2021. Urban heat island: causes, consequences, and mitigation measures with emphasis on reflective and permeable pavements. CivilEng. 2673-4109. 2 (2), 459–484. doi:10.3390/civileng2020026.

Wang, Y.C., Hu, B.K.H., Myint, S.W., Feng, C.C., Chow, W.T.L., Passy, P.F., 2018. Patterns of land change and their potential impacts on land surface temperature change in Yangon, Myanmar. Sci. Total Environ. 18791026. 643, 738–750. Available from: www.elsevier.com/locate/scitotenv. doi:10.1016/j.scitotenv.2018.06.209.

Xu, X., Sun, S., Liu, W., García, E.H., He, L., Cai, Q., Xu, S., Wang, J., Zhu, J., 2017. The cooling and energy saving effect of landscape design parameters of urban park in summer: a case of Beijing, China. Energy Build. 03787788. 149, 91–100. doi:10.1016/j.enbuild.2017.05.052.

Xue, Z., Hou, G., Zhang, Z., Lyu, X., Jiang, M., Zou, Y., Shen, X., Wang, J., Liu, X., 2019. Quantifying the cooling-effects of urban and peri-urban wetlands using remote sensing data: case study of cities of Northeast China. Landsc. Urban Plan. 01692046. 182, 92–100. doi:10.1016/j.landurbplan.2018.10.015.

Zaid, H.A.B., Mughal, U.M., Amin, M., Sajjad, M.M., Farhan, M., Sattar, A., Ali, S., Ali, M., Ain, Q.U., 2025. Evaluating the cooling potential of urban green spaces in Faisalabad integrating invest urban cooling model with multisource remote sensing data. Theor. Appl. Climatol. 14344483. 156 (9). Available from: https://www.springer.com/journal/704. doi:10.1007/s00704-025-05694-7.

Zardo, L., Geneletti, D., Pérez-Soba, M., Van Eupen, M., 2017. Estimating the cooling capacity of green infrastructures to support urban planning. Ecosyst. Serv. 22120416. 26, 225–235. doi:10.1016/j.ecoser.2017.06.016.

Zawadzka, J.E., Harris, J.A., Corstanje, R., 2021. Assessment of heat mitigation capacity of urban greenspaces with the use of InVEST urban cooling model, verified with day-time land surface temperature data. Landsc. Urban Plan. 01692046. 214, 104163. doi:10.1016/j.landurbplan.2021.104163.

Zomer, R., Trabucco, A., 2019. Global Aridity Index and Potential Evapotranspiration (ET0) Database: Version 3.1. figshare. Dataset. doi:10.6084/m9.figshare.7504448.v3.